

Novel positron acceleration by continuous coherent mid-infrared radiation in a micro-tube

Meiyu Si,^{1,2,3} Yongsheng Huang,^{2*} Manqi Ruan,¹ Baifei Shen,⁴ Zhangli Xu,⁴
Tongpu Yu,⁵ Xiongfei Wang,^{6,7} Yuan Chen,⁸

¹Institute of High Energy Physics, Chinese Academy of Sciences, Beijing 100049, China

²School of Science, Shenzhen Campus of Sun Yat-sen University, Shenzhen 518107, China

³University of Chinese Academy of Sciences, Beijing 100049, China

⁴Department of Physics, Shanghai Normal University, Shanghai 200234, China

⁵Department of Physics, National University of Defense Technology, Changsha 410073, China

⁶School of Physical Science and Technology, Lanzhou University, Lanzhou 730000, China

⁷Lanzhou Center for Theoretical Physics, Laboratory of Theoretical Physics of Gansu Province and Frontiers Science Center for Rare Isotopes, Lanzhou University, Lanzhou 730000, China

⁸The Institute for Advanced Studies of Wuhan University, 299, Bayi Road, Wuhan 430072, China

* E-mail: huangysh59@mail.sysu.edu.cn.

Efficient particles acceleration technology is of unique significance to the exploration of elementary particles, defeating cancer, and developing new materials. With the injection of the relativistic electron beam into the micro-tube, the strong transverse self-consistent field acts on the inner-wall of the plasma or the metal tube and causes the surface-nanometer electron film to oscillate in and out of the surface. Due to the mid-infrared radiation from the oscillating electrons continuously, a stable and periodic intense field of about tens of GV/m, propagates synchronously with the electron beam and accelerates the positron bunch in a stable phase. The acceleration scheme can realize cas-

cade acceleration of a single positron bunch and series acceleration of multiple positron bunches easily, making it possible to accelerate positron bunch continuously, stably and efficiently.

Introduction

High efficiency particles acceleration technology has unique significance in particles physics, materials science, laboratory astrophysics, medical physics (1–3). Different from conventional accelerators limited by material ionization threshold (4, 5), the plasma wakefield acceleration (PWFA) of electrons has achieved great progresses on the ultra-intense acceleration field and the controlling of the energy spread and the beam emittance (6–10). The great success of PWFA has stimulated the strong desire for high-field gradient positron acceleration with various plasma-dominated schemes (11–28). Among them, the stable field structure driven by an electron beam (21–26, 28) or a proton beam (17) in a hollow channel is potentially leading to high efficiency and narrow energy spread positron acceleration. Taking a different approach, ultra-short electron beam driven coherent transition radiation (CTR) can also accelerate the self-generated positron bunch in the interaction between the short beam and the copper film (20). Although a strong magnetic field (20) or a proper waveguide (29) was used to try to solve the fast divergence of CTR and the electron beam, however, the energy transfer efficiency was still quite low. In this paper, we propose a novel mechanism in which intense coherent mid-infrared radiation can emit continuously from the surface-nanometer electron film oscillations driven by a relativistic electron beam in a plasma micro-tube or metal micro-tube. Therefore, a stable high-efficient uniform field structure can be superimposed by the mid-infrared radiation field and the self-field of the relativistic electron beam and provides stable intense longitudinal force and weak transverse focusing force. Therefore, in this field, the injected positron bunch can be accelerated stably to several GeV and the energy spread can be preserved to be 1% level in

several centimeters. The energy transfer efficiency can reach 22% corresponding to the initial positron charge, 0.56 nC.

Similar with CTR from a short electron beam, the coherent mid-infrared radiation is also emitted from the oscillated surface-nanometer film continuously. With the injection of the relativistic electron beam into the micro-tube, the strong transverse self-consistent field acts on the inner-wall and causes the surface-nanometer electron film to oscillate in and out of the surface. Due to the mid-infrared radiation from the oscillating electrons continuously, a field of about tens of GV/m, propagates synchronously with the electron beam and accelerates the positron bunch in a stable phase. Figure 1A shows the periodically distributed mid-infrared radiation acceleration field generated by a relativistic electron beam propagation in the micro-tube. The radius of the micro-tube is $50 \mu\text{m}$ with the plasma thickness of $30 \mu\text{m}$. The green line is the acceleration field at $L_y = 0$. The longitudinal acceleration field is ultra-intense and of the order of tens of GV/m, which is uniform and stable, and has a high tolerance for the off-axis injection positron bunch. Figure 1, A1 and A2, which show the magnification of the first period region in Fig. 1A and the phase of the electrons and positrons. In this scheme, the radiation field is bound by the electron beam and propagates synchronously with it. The electron beam energy is transferred to the positron beam through the continuous coherent mid-infrared radiation field of surface-nanofilm-plasma oscillations. The acceleration of a positron bunch in a solid-density-plasma micro-tube structure is simulated. The detailed parameters of simulation are described in the materials and methods in supplementary materials. Figure 1, B and C, which show the density distribution of electrons and positrons at $t = 117 \text{ ps}$, respectively. The electron bunch experiences longitudinal deceleration and weak transverse defocus in the process of motion. While in the same phase, the positron bunch experiences longitudinal acceleration and weak transverse focus. It is clear that the longitudinal scale of the electron bunch is stretched, and the positron bunch is compressed. The energy-space distribution of the electrons and positrons

with the initial energy of 1 GeV and 5 GeV are shown in Fig. 1, D and E, respectively.

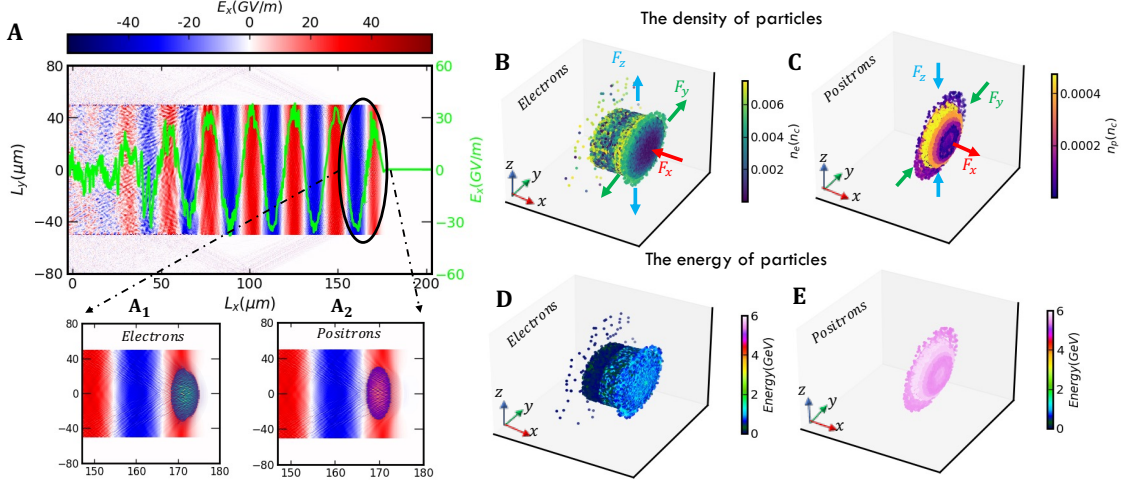


Fig. 1. A novel scheme for positron bunch acceleration in a micro-tube. (A) The periodically distributed mid-infrared radiation acceleration field generated by a relativistic electron beam propagation in a micro-tube. The acceleration gradient can reach tens of GV/m. The electron beam energy is transferred to the positron beam through the continuous coherent mid-infrared radiation field of surface-nanofilm-plasma oscillations in and out of inner surface of the tube. (B) The density distribution of electrons at $t = 117$ ps. The electron bunch experiences longitudinal deceleration and weak transverse defocus. While the same phase, the density distribution of positrons is shown in (C). The positron bunch experiences longitudinal acceleration and weak transverse focus. (D) The energy-space distribution of the electrons with the initial energy of 1 GeV, and (E) the energy-space distribution of the positrons with the initial energy of 5 GeV show the stable acceleration structure at $t = 117$ ps.

The acceleration results show that the positron bunch can obtain high energy gain of about 1 GeV at the distance of about 4 cm and can maintain low energy spread smaller than 2%. Figure 2A shows the relationship between the acceleration time and the positron energy and the relative energy spread. The positron bunch accelerates from an initial average energy of 5 GeV to 6 GeV within 140 ps. And the relative energy spread of positron bunch is 1.9%. In the process of acceleration, Fig. 2B shows the decrease of the total charge of electron beam and positron bunch during acceleration. The initial energy of electron beam is 1 GeV with a 3.404

nC beam charge. Two cases are shown for the positron bunches with different initial energy of 1 GeV and 5 GeV and the same beam charge of 0.11 nC. Figure 2C shows the final energy spectrum of positron bunches with different initial energy and the electron beam at 140 ps. The energy transfer efficiency from the driving electron beam to the positron bunch is defined as $\eta = (\delta E_p \cdot Q_p) / (\delta E_e \cdot Q_e)$, where $\delta E_{e/p}$ is the energy change value of electron or positron bunch and $Q_{e/p}$ is the charge of the electron or positron bunch. The energy transfer efficiency about 3% for the initial energy 1 GeV and 5% for the initial energy 5 GeV of the positron bunch. The energy transfer efficiency, η , increases with the initial charge of positron bunch, n_p , and can even reach 40% if $n_p = 1.8$ nC in Fig. 2D. The self-consistent fields of the relativistic electron beam in plasma micro-tube and the intense continuous coherent mid-infrared radiation generated by surface-nanofilm-plasma oscillations are analyzed. In the uniform mid-infrared radiation field, the transverse field ($E_y - cB_z$) focuses the positron bunch within the early twenty picoseconds and finally weakly defocuses it until the transverse field decreases to zero due to the energy loss and beam break of the driven electron beam. Through lots of two-dimensional particle-in-cell (PIC) simulation, the transverse spatial misalignment of the positron injection is allowed to be a few microns if 17% relative loss of the energy transfer efficiency is accepted, where the accelerated energy and the energy spread are hardly affected. The design scheme of cascade acceleration of a single positron bunch and series acceleration of multiple positron bunches are discussed.

Analysis of e^+ acceleration process

Self-consistent fields of the relativistic e^- beam in a plasma micro-tube

For a relativistic electron beam propagating in the x direction in a free space at a normalized velocity $V_x = \beta_0$ with assigned density distribution ρ_b , the initial current is $J(x, t = 0) = \beta_0 \rho_b$. To compute the self-consistent fields at the initial time, we need to solve the electrostatic

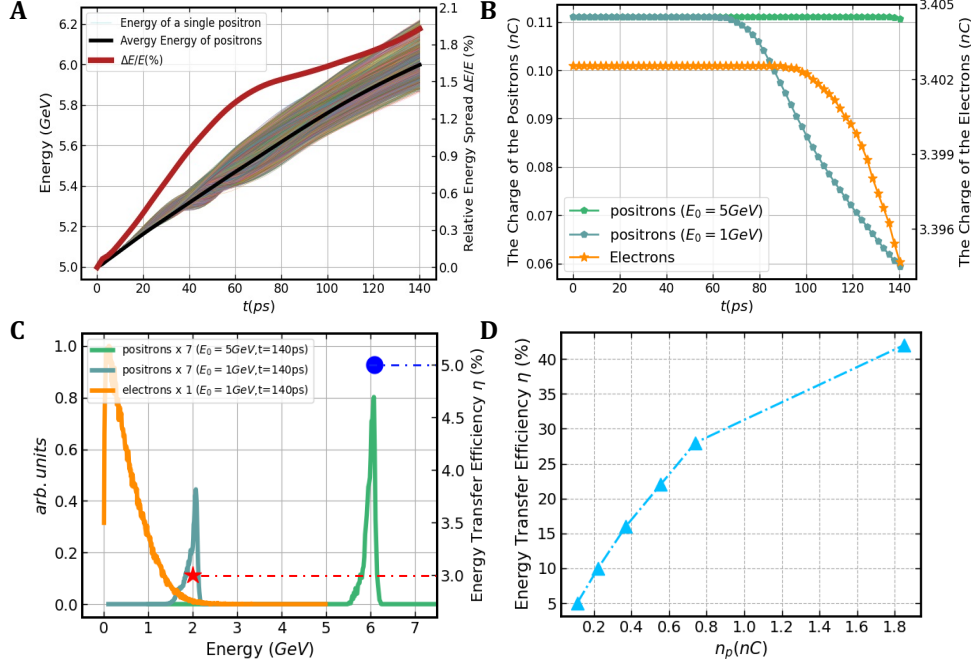


Fig. 2. The simulation results of e^+ acceleration in a micro-tube. (A) The relationship between the acceleration time and the positron energy and the relative energy spread. At the acceleration distance of 4.2 cm, the average energy gain of positrons is 1 GeV. The relative energy spread of positron bunch is 1.9%. (B) The decrease of the total charge of electron and positron bunch during acceleration. The initial energy of electron beam is 1 GeV with a 3.404 nC beam charge. Two cases are shown for the positron bunches with different initial energy of 1 GeV and 5 GeV and the same beam charge of 0.11 nC. (C) The final energy spectrum of the positron bunches with different initial energy and the electron beam at $t = 140$ ps. (D) The energy transfer efficiency, η , increases with the initial charge of positron bunch, n_p , and can even reach 40% if $n_p = 1.8$ nC.

potential in a Lorentz frame moving at speed β_0 (30, 31). In the relativistic species rest frame, the charge distribution is static and the electrostatic potential is related to the charge density through the Poisson's equation:

$$\nabla'^2 \Phi'^2 = -\rho' \quad (1)$$

where $\nabla' = \partial_{x'}^2 + \partial_{y'}^2 + \partial_{z'}^2$ is the Laplacian operator, $\Phi' = \Phi/\gamma_0$ is the bunch potential, $\rho' = \rho_b/\gamma_0$ is the density of the electron beam. $\gamma_0 = 1/\sqrt{1 - \beta_0^2}$ is the Lorentz factor of the relativistic electron beam. According to the Lorentz back-transformation of coordinates, the

relativistic Poisson's equation in the laboratory frame can be written as (32):

$$\left[\frac{1}{\gamma_0^2} \frac{\partial^2}{\partial x^2} + \frac{\partial^2}{\partial y^2} + \frac{\partial^2}{\partial z^2} \right] \Phi = -\rho_b \quad (2)$$

In order to solve the initial potential Φ in a free space, the standard FFT algorithm is used to realize the cosine transform. Therefore, the electric fields of the initial electron beam can be computed as follows:

$$E_x = -\frac{1}{\gamma_0^2} \partial_x \Phi, E_y = -\partial_y \Phi \quad (3)$$

Due to the $1/\gamma_0^2$ factor, the longitudinal electric field E_x will be much smaller than the transverse electric field E_y . The distribution of the initial electric fields are obtained by a PIC simulation for a Gaussian electron bunch of charge 3.265 nC, the longitudinal rms-length σ_x is 3.3 μm , the transverse rms-length σ_r is 26.9 μm , where $r = \sqrt{y^2 + z^2}$. The relativistic factor $\gamma_0 \approx 1957$ for the electron energy, 1 GeV. The initial longitudinal electric field E_x and transverse electric field E_y of the relativistic electron beam are shown in Fig. 3, A and B, respectively. The subgraph in (A) and (B) show the electrostatic field of a static electron beam. The transverse field of the relativistic electron beam at $L_y = 50 \mu\text{m}$ is about 200 GV/m and is larger than that of a static electron bunch. Therefore, the strong transverse field E_y of the moving electron beam is applied to the plasma inner-wall in micro-tube and decays exponentially in the solid-density-plasma film, which can be written as E_{yp} in Eq. (4).

$$E_{yp} = E_0 e^{-\sqrt{k_x^2 - 1 + \omega_{pe}^2} \delta y}, \delta y = y' - r \quad (4)$$

where r is the radius of plasma micro-tube and y' is the penetration depth of the E_y field in the plasma. The plasma frequency is $\omega_{pe} = \sqrt{4\pi e^2 \rho / m} \approx 5.6 \times 10^{15}$ Hz, where ρ is the density of dense plasma micro-tube. The longitudinal length of the electron beam is λ about 7 μm . The normalized parameters is $\omega_L = 2\pi c / \lambda$, $L = c / \omega_L \times 10^6 (\mu\text{m})$. The surface-nanometer electron film was pushed away to form a strong charge separation field, which is proportional to the

separation distance and is written in Eq. (5).

$$E_{cs} = \frac{e}{\epsilon_0} \cdot \rho \cdot \delta y \quad (5)$$

Figure 3C shows the strong transverse field distribution of a relativistic electron beam propagating in a solid-density-plasma micro-tube with the radius of 50 μm . For $y > 0$, the surface-nanometer electron film (δ_y) is first pushed away in the region, $F > 0$ then pulled back in the region, $F < 0$, where F is the resultant force of the two forces $F_{yp} = -eE_{yp}$ and $F_{cs} = -eE_{cs}$, indicating the oscillation of the nanometer-plasma electrons. Figure 3D shows the distribution of the electric field in dense plasma E_{yp} and the charge separation field E_{cs} . At $\delta_y = 1.1$ nm, $F = 0$ and the plasma electrons gain the maximum momentum.

Intense continuous coherent mid-infrared radiation from surface-nanofilm-plasma oscillations

The combined force, F , of the electric field E_{yp} in the solid-density-plasma and the charge-separation field E_{cs} make the surface-nanometer electron film oscillation in and out of the surface. The energy of the surface-plasma electrons can be obtained by:

$$\int_0^{\delta_y} (eE_{yp} - eE_{cs})dy = (\gamma_p - 1)m_e c^2 \quad (6)$$

For $\delta_y = 1.1$ nm, the γ_p is about 1.0002 and the velocity β_p is equal to 0.0206. Figure 4A shows the momentum distribution of the surface-plasma electrons by the PIC simulation. The region where the momentum reach maximum correspond to the region where the driven beam is being. The maximum momentum of plasma electrons is about 0.016 $m_e c$, which is in good agreement with the theoretical estimate. With the initial momentum, the surface-nanometer electron film begins to oscillate and generate continuous coherent mid-infrared radiation. For $\dot{\vec{\beta}}_p / \vec{\beta}_p$, the radiation field E_{rad} of an electron can be obtained as follows:

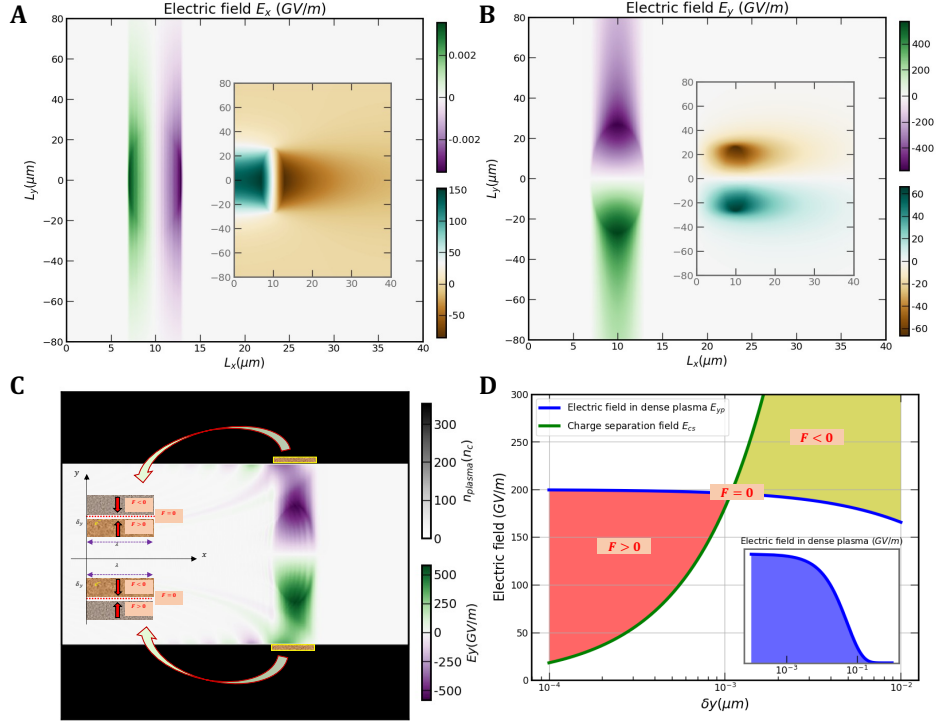


Fig. 3. Self-consistent fields of a relativistic electron beam in a solid-density-plasma micro-tube. (A) and (B) show the initial longitudinal electric field E_x and transverse electric field E_y of the relativistic electron beam, respectively. The subgraph shows the field of a static electron beam. The transverse field of the relativistic electron beam is larger than that of a static electron beam. (C) The strong transverse field of a relativistic electron beam at the surface of the micro-tube is still hundreds of GV/m and interacts with the plasma inner-wall, causing the surface-nanometer electron film to oscillate. (D) The combined force, F , of the electric field E_{yp} in dense plasma and the charge separation field E_{cs} determine the oscillation of the nanometer-plasma film.

$$E_{rad} = \frac{e}{4\pi\epsilon_0} \left[\frac{\vec{n} \times (\vec{n} \times \dot{\vec{\beta}}_p)}{c(1 - \beta_p \cos\theta)^3 R} \right] \quad (7)$$

where $\dot{\vec{\beta}}_p = e\vec{E}/(cm_e\gamma_p^3)$. θ is the angle between the solid angle direction \vec{n} and the velocity $\vec{\beta}_p$.

For the interaction region, the total radiation field E_{rad}^{tot} is calculated by integration $\int \rho dx dy dz$.

Therefore, the simplified expression of total radiation field E_{rad}^{tot} can be obtained as follows:

$$E_{rad}^{tot} = \int E_{rad}^x \rho x d\varphi dx dy = \frac{e\dot{\vec{\beta}}_p \rho \delta_y y}{2\epsilon_0 c} \int_0^\theta \frac{\sqrt{1 - \cos^2\theta \sin^2\theta}}{(1 - \beta_p \cos\theta)^3 \cos^2\theta} d\theta \quad (8)$$

where $E_{rad}^x = E_{rad}\sin\theta$ is the longitudinal radiation field, $y = R\cos\theta$ is distance from reference point to the micro-tube wall, $L_y = 50 \mu\text{m}$. The parameters required for calculation are shown in Table S1. Therefore, the total radiation field is obtained and the value is about tens of GV/m. As example, for $y = 1 \mu\text{m}$, the E_{rad}^{tot} is about 38 GV/m. Figure 4B shows the radiation field distribution in plasma micro-tube with the PIC simulation, the subgraph is the size of the radiation field at the $L_y = 50 \mu\text{m}$. With the relativistic electron beam propagating in the micro-tube, the continuous mid-infrared radiation evolves into the intense stable period acceleration field as shown in Fig. 1A. For the solid-density-plasma micro-tube with the radius $50 \mu\text{m}$, the pulse width of the stable period radiation field is about 0.4 ps. The transverse field is proportional to the charge of the relativistic electron beam and effect on the energy of the surface-nanometer-plasma, which results the radiation field. Figure 4C shows the variation of the acceleration electric field with the charge of the electron beam. Therefore, the acceleration gradient of positron bunch acceleration can be improved by increasing the charge of the initial driving electron beam.

Evolution of transverse field in the y direction

The stable acceleration of the positron bunch is achieved by the intense longitudinal acceleration field generated by the oscillation of surface-nanometer electron film in a plasma micro-tube. At the same time, the transverse self-generated field of the relativistic driven electron beam can provide a transverse focusing force on the positron bunch. The transverse fields in the y direction, $E_y - cB_z$ and $E_z + cB_y$ in the z direction are symmetric in simulation. Therefore, it is analyzed that the transverse field distribution and transverse motion of the positron bunch in the y direction, which goes through the first stage, weakly focusing and the second stage, weakly defocusing until the transverse fields decrease to zero.

Figure 5A shows the transverse field distribution of positron bunch at 0.1 ps, 1.9 ps, 21

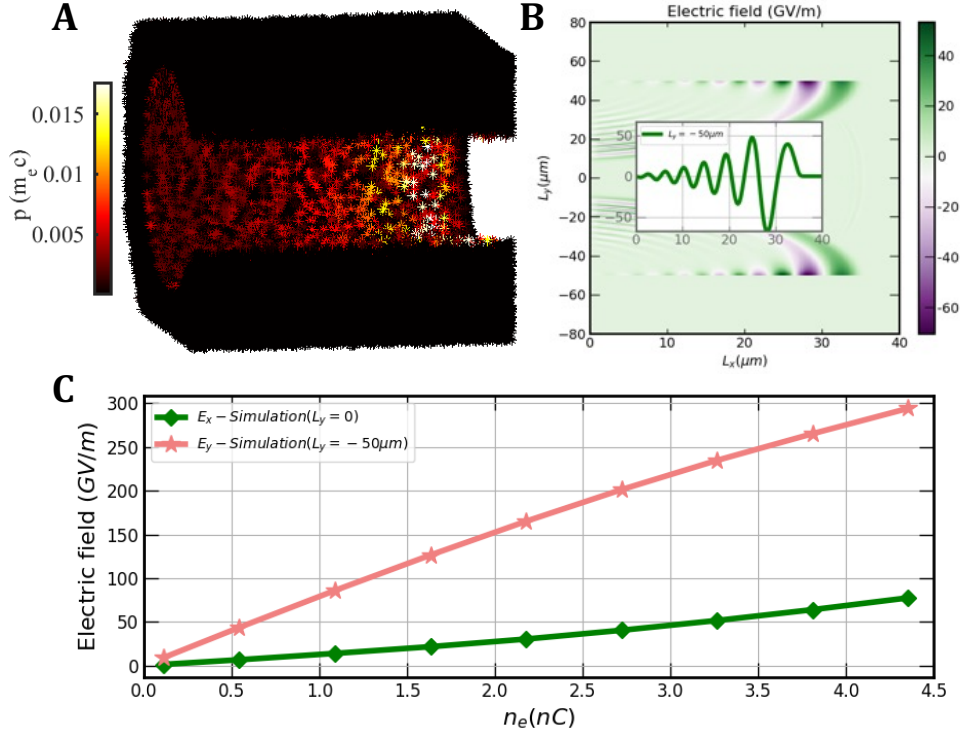


Fig. 4. An intense continuous coherent mid-infrared radiation field formed in the plasma micro-tube. (A) The momentum distribution of the surface-plasma electrons. Only the electrons in the surface-nanometer film gain kinetic energy. In the region after the electron beam passes through, the oscillations of the surface-nanometer electron film become weakened and the velocity decreases. (B) The radiation field distribution in plasma micro-tube with a radius of $50 \mu\text{m}$, the subgraph is the field at the radius of about tens of GV/m. (C) The variation of the acceleration electric field with the amount of charge of driving electron beam.

ps and 93 ps, respectively. In the early stage of the longitudinal acceleration, $t < 21$ ps, the transverse force is always focused. The electron beam in the same phase is constantly consumed, and its energy is transferred to the positron bunch through the radiation acceleration field, resulting in the weakening of transverse self-field. After 21 ps, the transverse field edge becomes uniform and the positron bunch can remain stable transversely for several tens of picoseconds. After that, it will be in a weak defocus field, where the transverse field will weaken until it is equal to zero due to the consumption of the driving electron beam.

Figure 5B shows the phase-space distribution of the positron bunch corresponding to the

case of transverse field distribution in Fig. 5A. The relativistic positron bunch is always in the weak field region which reduces the influence of transverse instability on the acceleration quality.

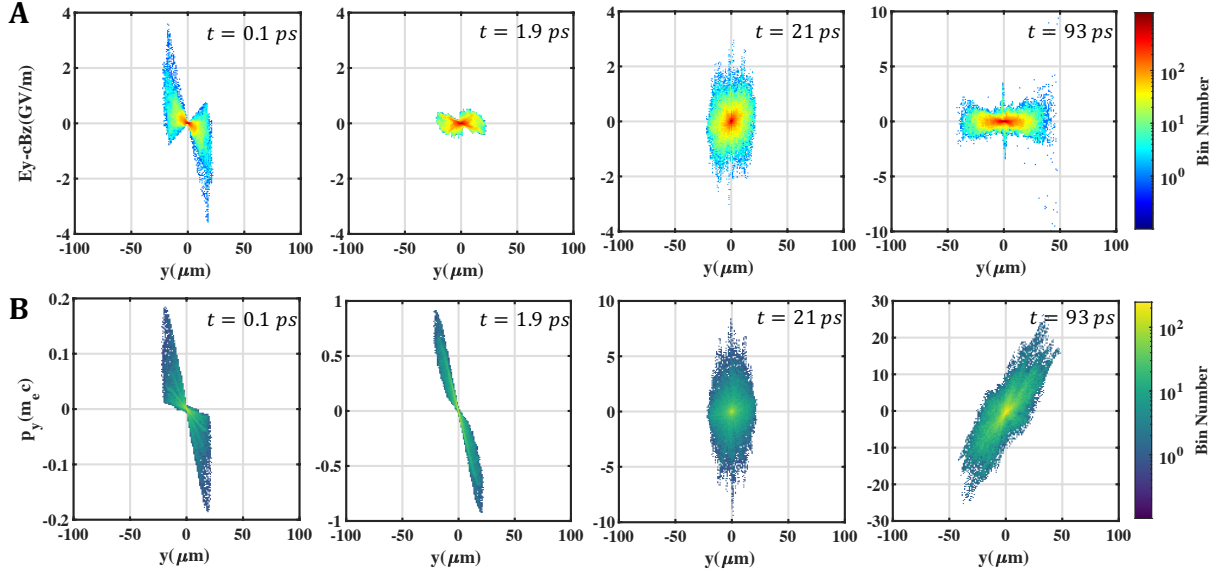


Fig. 5. Transverse field ($E_y - cB_z$) distribution experienced by positron bunch during acceleration of plasma micro-tube. (A) The transverse field distribution of positron bunch at 0.1 ps, 1.9 ps, 21 ps and 93 ps, respectively. The positron bunch is always in the weak field region. In the early stage of longitudinal acceleration, the positron bunch is transversely focused. After 21 ps, the transverse field edge becomes uniform and the positron bunch can remain stable for several tens of picoseconds. After that, it will be in a weak defocus field, and the transverse field guided by the driving electron beam will weaken until it equal to zero. **(B)** The phase-space distribution of the positron bunch corresponding to the case of the field distribution in **(A)**.

Analysis of transverse off-axis injection of positron bunch

The proposed novel acceleration scheme can achieve the stable and efficient acceleration of the externally injected positron bunch. Due to the uniformity of the acceleration field, the misalignment of the positron injection is inevitable experimentally but is allowed in a certain region. In order to find the acceptable misalignment, several two-dimensional PIC simulations were

performed for the transverse injection deviation from the central axis are $0 \mu\text{m}$, $5 \mu\text{m}$ and $10 \mu\text{m}$, respectively. The key points of the simulation are shown in the following parameters: the longitudinal and transverse size of the electron beam is $3.3 \mu\text{m}$ and $26 \mu\text{m}$ with density $1 \times 10^{24} \text{ m}^{-3}$, the longitudinal and transverse size of the positron bunch is $2 \mu\text{m}$ and $22 \mu\text{m}$ with density $7 \times 10^{21} \text{ m}^{-3}$. The initial injection position of the positron bunch is $y_0 = 0 \mu\text{m}$, $y_0 = 5 \mu\text{m}$ and $y_0 = 10 \mu\text{m}$, respectively. Other simulation parameters are the same as those of cylindrical coordinate simulation in materials and methods. Figure 6A shows the asymmetric phase-space distribution of positron bunch with ten micrometer positive y-axis deviation compared with the symmetric one. Figure 6B shows the density distribution of positron bunch in the xy plane after a long period of acceleration in both cases. Due to the initial injection deviation in y direction, although the phase-space distribution of the positron bunch maintains this asymmetry during the acceleration process, the central energy and the energy spread of the accelerated positron bunch are hardly affected in the uniform longitudinal acceleration field. Figure 6C shows the influence of different transverse injection misalignment, $y_0 = 0 \mu\text{m}$, $y_0 = 5 \mu\text{m}$ and $y_0 = 10 \mu\text{m}$, on the accelerated energy spectrum of positron bunch. The positron bunch gains the same amount of energy at the same time, however, the difference is the peak charge at the central energy, which affects the energy transfer efficiency η . The energy transfer efficiency of the accelerated positron bunch decreases by about 17% for the deviation of $10 \mu\text{m}$ relative to that without deviation. Therefore, the great tolerance for the injection deviation of the positron bunch greatly reduces the difficulty of the experimental implementation.

Discussions

In our model, the plasma density of the micro-tube is of the same order as the free-electron density in metals. In a metal micro-tube, our proposal is the same applicable. The transverse self-generated field E_y of the relativistic electron beam of several hundred GV/m can directly

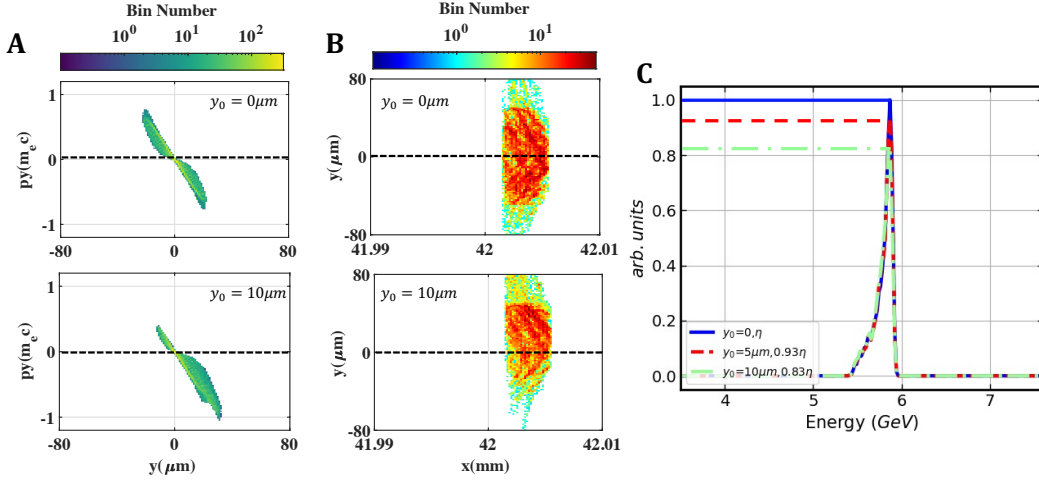


Fig. 6. The influence of the injection deviation of positron bunch in the y direction on the final acceleration result. (A) The asymmetric phase-space distribution of positron bunch with ten micrometer positive y -axis deviation compared with the symmetric one. (B) The density distribution of positron bunch in the xy plane after a long period of acceleration in both cases. (C) The influence of different transverse injection misalignment, $y_0 = 0 \mu\text{m}$, $y_0 = 5 \mu\text{m}$ and $y_0 = 10 \mu\text{m}$, on the accelerated energy spectrum of positron bunch. The positron bunch gains the same amount of energy at the same time, however, the difference is the peak charge at the central energy, which affects the energy transfer efficiency η . The energy transfer efficiency of the accelerated positron bunch decreases by about 17% for the deviation of $10 \mu\text{m}$ relative to that without deviation.

ionize the surface of the metal micro-tube, and can also cointeract with the space-separation field to driven the oscillation of the ionized electron film and the intense continuous coherent mid-infrared radiation. The novel high-efficient scheme has high acceleration gradient, tens of GV/m , stable acceleration structure and can also realize cascade acceleration easily, making it possible to accelerate positron continuously, stably and efficiently. Figure 7A shows the two-cascade design of the injection of the electron and positron bunch using a three-bifurcated tube. Figure 7B shows a cone-shaped coupling tube covered by the magnetic field B . For the magnetic field $B = 1 \text{ T}$ and the initial energy 1 GeV of the electron or positron bunch, the deflection radius of particle bunch is $R = E/qvB$ about 3.3 m . The angle of deflection is $\theta \approx 1.8 \times 10^{-4} \text{ rad}$ for $t = 2 \text{ ps}$. After the deflection, the positron bunch is accelerated 4.2 cm in a straight

line in the micro-tube to obtain 1 GeV energy gain. Through the stable periodic structure of the mid-infrared radiation acceleration field in the micro-tube, the series acceleration can also be considered to obtain multiple high-energy positron bunches at the same time. The process is demonstrated by 2D PIC simulation. Figure 7C shows the radiation field driven by a single electron beam in a micro-tube accelerating three positron bunches simultaneously, including $x_{positrons}^{(1)}$, $x_{positrons}^{(2)}$, $x_{positrons}^{(3)}$, with initial positions of 178 μm , 158 μm and 135 μm , respectively. The detailed diagram of the beam density distribution can be obtained in Fig. S1. Therefore, each of the three positron bunches obtains about 1 GeV energy gain at an accelerated distance of 4 cm. The final energy spectrum of the positron bunches is shown in Fig. 7D with the initial energy of 5 GeV. The energy transfer efficiency is about 3-4 times higher than that of a single positron bunch acceleration. Due to the effect of the electron beam in the first period, the radiation field in the second and third periods is more stable and the acceleration of the positron bunch is better than the positron bunch in the first period. More detailed research is necessary in the next step, including the injection of multiple particle beams.

Conclusion

In this paper, we propose a novel scheme for the acceleration of positron bunch in which intense coherent mid-infrared radiation can emit continuously from the surface-nanometer electron film oscillations driven by a relativistic electron beam in a plasma micro-tube or metal micro-tube. Therefore, a stable high-efficient uniform field structure can be superimposed by the radiations field and the self-field of the relativistic electron beam and provides stable intense longitudinal force and weak transverse focusing force. As an example, the positron bunch can obtain 1 GeV energy gain at the distance of about 4 cm and can maintain low energy spread smaller than 2%. The electron beam energy is transferred to the positron bunch through the continuous coherent mid-infrared radiation field from surface-nanofilm-plasma oscillations. The energy transfer

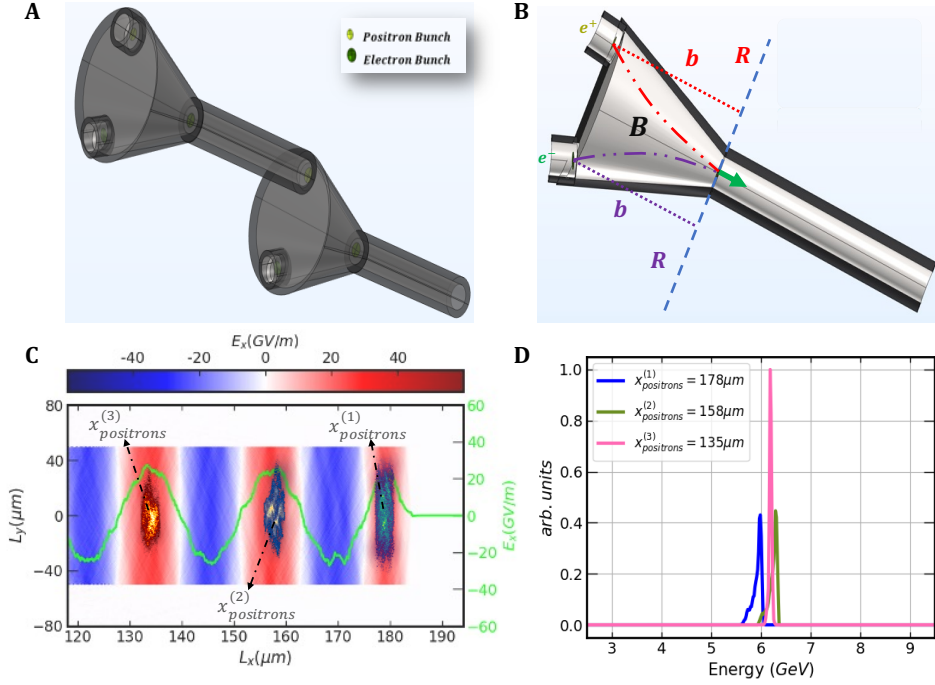


Fig. 7. The schematic diagram of cascade acceleration of a single positron bunch and series acceleration of multiple positron bunches. (A) The two-cascade design of the injection of the electron and positron bunch using a three-bifurcated tube. (B) A cone-shaped coupling tube covered by the magnetic field B . R is the radius of deflection. For the magnetic field $B = 1$ T and the initial energy 1 GeV of the electron or positron bunch, the deflection radius of particle bunch is $R = E/qvB$ about 3.3 m. (C) The mid-infrared radiation field driven by a single electron beam in a micro-tube accelerating three positron bunches simultaneously, including $x_{positrons}^{(1)}$, $x_{positrons}^{(2)}$, $x_{positrons}^{(3)}$, with initial positions of 178 μm , 158 μm and 135 μm , respectively. (D) The final energy spectrum of the positron bunches with the initial energy of 5 GeV at $t = 140$ ps.

efficiency η about 5% of 0.11 nC positron bunch and 22% of 0.56 nC positron bunch. In the uniform mid-infrared radiation field, the transverse field ($E_y - cB_z$) focuses the positron bunch within the early twenty picoseconds and finally weakly defocuses it until the transverse field decreases to zero due to the energy loss and beam break of the driven electron beam. The great tolerance for the injection deviation of the positron bunch greatly reduces the difficulty of the experimental implementation. Through lots of two-dimensional PIC simulation, the transverse spatial misalignment of the positron injection is allowed to be a few microns if 17% relative

loss of the energy transfer efficiency is accepted, where the accelerated energy and the energy spread are hardly affected. The plasma density of the micro-tube is of the same order as the free-electron density in metals. In a metal micro-tube, our proposal is the same applicable. The novel high-efficient scheme has high acceleration gradient, tens of GV/m, stable acceleration structure and can also realize cascade acceleration easily, making it possible to accelerate positron bunch continuously, stably and efficiently. We can also consider using this method to realize the series acceleration of positron bunch and obtain several high-energy positron bunches at the same time.

Acknowledgments

Funding: This work is supported in part by National Natural Science Foundation of China (11655003); Innovation Project of IHEP (542017IHEPZZBS11820, 542018IHEPZZBS12427); the CAS Center for Excellence in Particle Physics (CCEPP); IHEP Innovation Grant (Y4545170Y2); Chinese Academy of Science Focused Science Grant (QYZDY-SSW-SLH002); Chinese Academy of Science Special Grant for Large Scientific Projects (113111KYSB20170005); National 1000 Talents Program of China; the National Key Research and Development Program of China (No.2018YFA0404300); National Natural Science Foundation of China (Grant No. 11975252); Youth Innovation Promotion Association CAS (No. 2021012). **Author contributions:** M.Y.S. contributed to investigation, validation, formal analysis, data curation, simulation, writing—original draft. Y.S.H. contributed to conceptualization, methodology, formal analysis, supervision, project administration, funding acquisition, writing—review and editing. M.Q.R. contributed to formal analysis. B.F.S. contributed to formal analysis. Z.L.X. helped in formal analysis. T.P.Y. helped in formal analysis. X.F.W. contributed to formal analysis. Y.C. contributed to formal analysis. **Competing interests:**The authors declare no conflicts of interest. **Data and materials availability:** This manuscript has no associated data or the data will not be deposited.

Methods

The proposed scheme is confirmed by cylindrical geometry with a decomposition in azimuthal modes using the SMILEI (33) code, which is an open-source, user-friendly, high-performance and multi-purpose electromagnetic PIC code for plasma simulation. The grid coordinates are two-dimensional (x, r), while particle coordinates are expressed in the three-dimensional Cartesian frame (x, y, z). A moving window of $51.2 \mu\text{m} (L_x) \times 100 \mu\text{m} (L_r)$ is used and sampled by $512 (x) \times 400 (r)$ cells. The plasma critical number density n_c is $2.82 \times 10^{25} \text{ m}^{-3}$. The density of the dense plasma is 10^{28} m^{-3} with the radius of $50 \mu\text{m}$ and the thickness of $30 \mu\text{m}$. For $0 < r < 50 \mu\text{m}$, the rarefied gas is filled with density of 10^{21} m^{-3} . The initial energy of the driving electron bunch is 1 GeV, with a 3.404 nC beam charge. The initial momentum is Maxwell-Juttner distribution with temperature $0.1 m_e c^2$ in the x direction and $0.001 m_e c^2$ in the y and z direction. The density profile of the electron bunch is a Gaussian distribution in the x and r direction, $n_e = n_{e0} e^{-(x-x_0)^2/\sigma_{xe}^2} \cdot e^{-(r)^2/\sigma_{re}^2}$, where $n_{e0} = 4 \times 10^{24} \text{ m}^{-3}$, $x_0 = 5 \mu\text{m}$, longitudinal rms-length $\sigma_{xe} = 3.3 \mu\text{m}$, transverse rms-length $\sigma_{re} = 26 \mu\text{m}$, where $r = \sqrt{y^2 + z^2}$. The witness positron bunch has an initial energy of 5 GeV or 1 GeV and a beam charge of 0.11 nC. The density of the positron bunch is $n_p = 3 \times 10^{23} \text{ m}^{-3}$ with longitudinal rms-length $\sigma_{xp} = 2 \mu\text{m}$, transverse rms-length $\sigma_{rp} = 22 \mu\text{m}$. The initial energy spread, angular distribution and the normalized emittances of the positron bunch is neglected. There are 20 macro-particles per cell (PPC) for the driving electron bunch and the witness positron bunch, and 4 PPC for the plasma species. The result has been compared with PPC=50 for particles bunch and PPC=4/100/200/400 for the plasma particles of micro-tube, which are almost no difference. In order to save computational costs, the above parameters are selected.

References and Notes

1. L. Marchut, C. J. McMahon, Electron and positron spectroscopies in materials science and engineering. *Electron Positron Spectroscopies in Materials Science Engineering*, 1–33 (1979).
2. Guessoum, Nidhal, Positron astrophysics and areas of relation to low-energy positron physics. *European Physical Journal D* 68, 1-6 (2014).
3. K. R. Hogstrom, P. R. Almond, Review of electron beam therapy physics. *Physics in Medicine, Biology* 51, R455 (2006).
4. E. Gschwendtner, P. Muggli, Plasma wakefield accelerators. *Nature Reviews Physics* 1, 246-248 (2019).
5. X. J. Jiao, J. M. Shaw, T. Wang et al, A tabletop, ultrashort pulse photoneutron source driven by electrons from laser wakefield acceleration. *Matter and Radiation at Extremes* 2, 296-302 (2017).
6. T. Tajima, J. M. Dawson, Laser electron accelerator. *Physical Review Letters* 43, 267 (1979).
7. Katsouleas, Thomas, Electrons hang ten on laser wake. *Nature* 431, 515-516 (2004).
8. J. Faure, Y. Glinec, A. Pukhov et al, A laser–plasma accelerator producing monoenergetic electron beams. *Nature* 431, 541-544 (2004).
9. S. P. Mangles, C. D. Murphy, Z. Najmudin et al, Monoenergetic beams of relativistic electrons from intense laser–plasma interactions. *Nature* 431, 535-538 (2004).
10. C. G. R. Geddes, C. Toth, J. Van Tilborg et al, High-quality electron beams

- from a laser wakefield accelerator using plasma-channel guiding. *Nature* 431, 538-541 (2004).
11. T. J. Xu, B. F. Shen et al, Ultrashort megaelectronvolt positron beam generation based on laser-accelerated electrons. *Physics of Plasmas* 23, 033109 (2016).
 12. X. L. Zhu, M. Chen, T. P. Yu et al, Collimated GeV attosecond electron–positron bunches from a plasma driven by 10 PW lasers. *Matter and Radiation at Extremes* 4, 014401 (2019).
 13. K. V. Lotov, Acceleration of positrons by electron beam-driven wakefields in a plasma. *Physics of Plasmas* 14, 023101 (2007).
 14. C. Du, Z. Xu, Positron acceleration by a laser pulse in a plasma. *Physics of Plasmas* 7, 1582-1585 (2000).
 15. H. Hasegawa, S. Usami, Y. Ohsawa, Positron acceleration to ultrarelativistic energies by a shock wave in a magnetized electron–positron–ion plasma. *Physics of Plasmas* 10, 3455-3458 (2003).
 16. X. Wang, R. Ischebeck et al, Positron Injection and Acceleration on the Wake Driven by an Electron Beam in a Foil-and-Gas Plasma. *Physical Review Letters* 101, 124801 (2008).
 17. L. Yi, B. Shen et al, Positron acceleration in a hollow plasma up to TeV regime. *Scientific Reports* 4, 4171 (2014).
 18. J. Vieira, J.T. Mendonça, Nonlinear laser driven donut wakefields for positron and electron acceleration. *Physical Review Letters* 112, 215001(2014).
 19. S. Zhou, J. Hua et al, High efficiency uniform wakefield acceleration of a positron beam using stable asymmetric mode in a hollow channel plasma.

- Physical Review Letters* 127, 174801(2021).
20. Z. Xu, L. Yi et al, Driving positron beam acceleration with coherent transition radiation. *Communications Physics* 3, 191 (2020).
 21. T. C. Chiou, T. Katsouleas et al, Laser wake-field acceleration and optical guiding in a hollow plasma channel. *Physics of Plasmas* 2, 310-318 (1995).
 22. T. C. Chiou, T. Katsouleas, High beam quality and efficiency in plasma-based accelerators. *Physical Review Letters* 81, 3411(1998):.
 23. C. B. Schroeder, D. H. Whittum, J. S. Wurtele, Multimode analysis of the hollow plasma channel wakefield accelerator. *Physical Review Letters* 82, 1177 (1999).
 24. C. B. Schroeder et al, Beam loading in a laser-plasma accelerator using a near-hollow plasma channel. *Physics of Plasmas* 20, 123115 (2013).
 25. S. Gessner, E. Adli et al, Demonstration of a positron beam-driven hollow channel plasma wakefield accelerator. *Nature communications* 7, 1-6 (2016).
 26. C. A. Lindstrøm, E. Adli et al, Measurement of transverse wakefields induced by a misaligned positron bunch in a hollow channel plasma accelerator. *Physical Review Letters* 120, 124802 (2018).
 27. N. Jain, T. M. Antonsen Jr, J. P. Palastro, Positron acceleration by plasma wakefields driven by a hollow electron beam. *Physical Review Letters* 115, 195001 (2015).
 28. S. Diederichs et al, Positron transport and acceleration in beam-driven plasma wakefield accelerators using plasma columns. *Physical Review Accelerators and Beams* 22, 081301 (2019).

29. Z. Xu et al, Positron acceleration by terahertz wave and electron beam in plasma channel.
30. P. Londrillo, C. Gatti, M. Ferrario, Numerical investigation of beam-driven PWFA in quasi-nonlinear regime. *Nuclear Instruments and Methods in Physics Research Section A: Accelerators, Spectrometers, Detectors and Associated Equipment* 740, 236-241 (2014).
31. F. Massimo, A. Marocchino, A. R. Rossi, Electromagnetic self-consistent field initialization and fluid advance techniques for hybrid-kinetic pwfa code architect. *Nuclear Instruments and Methods in Physics Research Section A: Accelerators, Spectrometers, Detectors and Associated Equipment* 829, 378-382 (2016).
32. A. Marocchino, E. Chiadroni et al, Design of high brightness Plasma Wake-field Acceleration experiment at SPARC-LAB test facility with particle-in-cell simulations. *Nuclear Instruments and Methods in Physics Research Section A: Accelerators, Spectrometers, Detectors and Associated Equipment* 909, 408-413 (2018).
33. J. Derouillat et al, SMILEI: A collaborative, open-source, multi-purpose particle-in-cell code for plasma simulation. *Computer Physics Communications* 222, 351-373 (2017).